Journal of Organometallic Chemistry 799-800 (2015) 195–200

Contents lists available at ScienceDirect

Journal of Organometallic Chemistry

journal homepage: www.elsevier.com/locate/jorganchem

Full functionalized silica nanostructure with well-defined size and functionality: Octakis(3-mercaptopropyl)octasilsesquioxane

Ana–Maria-Corina Dumitriu [a], Maria Cazacu [a, *], Alexandra Bargan [a], Mihaela Balan [a], Nicoleta Vornicu [b], Cristian-Dragos Varganici [a, c], Sergiu Shova [a]

[a] "Petru Poni" Institute of Macromolecular Chemistry, Aleea Gr. Ghica Voda 41A, Iasi, 700487, Romania
[b] Centre of Advanced Research in Bionanoconjugates and Biopolymers, "Petru Poni" Institute of Macromolecular Chemistry, Aleea Gr. Ghica Voda 41A, Iasi, 700487, Romania
[c] Metropolitan Center of Research T.A.B.O.R, The Metropolitanate of Moldavia and Bukovina, Closca 9, 700066, Iasi, Romania

ARTICLE INFO

Article history:
Received 15 December 2014
Received in revised form
12 August 2015
Accepted 20 September 2015
Available online 25 September 2015

Keywords:
Cubic polyhedral silsesquioxanes
Synthesis
Structural characterization
Functionalized silica
Nanosized structures

ABSTRACT

The acid hydrolysis of 3-mercaptopropyltrimethoxysilane resulted in the formation of cubic silsesquioxane **1** containing original organic function (SH). The structure was elucidated through X-ray single crystal diffraction, spectral (FTIR and NMR) techniques and elemental analysis. Values of the inner and outer diameter of the nanostructure of 0.54, 1.63 nm were found. Thermal behavior was investigated by thermogravimetric analysis (TGA) and differential scanning calorimetry (DSC), while that in dependence on moisture was assessed through water vapor sorption in dynamic regime (DVS). The biological activity of the compound was also tested.

1. Introduction

Completely condensed polyhedral oligosilsesquioxanes, abbreviated by the acronym POSSs are a group of nanometer-scaled organosilicon compounds with well-defined and highly symmetrical structures with the general formula $Si_nO_{3n/2}R_n$ or T_nR_n (where n = 4, 6, 8, 10, 12, R = H, or any alkyl, alkylene, aryl, arylene, and their organofunctional derivatives). These compounds are organic-inorganic architectures, with inner inorganic frameworks consisting of silicon and oxygen atoms surrounded by organic R substituents, in three dimensional arrangements [1–3]. The R groups determine many of the physical and chemical properties of the cage molecule [1] and may be the same or different, non-reactive or reactive. As a result, depending on the reactivity of the organic group R, POSSs can be classified as nonfunctional and functional. The latter is of greater interest since the reactive R groups permit the chemical bonding of the cages to different substrates [3]. The most representative members of this family are the cubic (n = 8), $R_8Si_8O_{12}$ or T_8, whose formation is favored by the steric effects [3–5]. The T_8 silsesquioxanes have been used as "nanobuilding blocks" into polymer networks, in nanoparticles, in optically active materials, for drug delivery, in nanocomposites, in liquid crystalline materials, as cores for dendrimers, flow aids for high temperature thermoplastics, etc. [7–9]. Some promising bio-inspired research areas for POSS include bone growth and soft tissue healing [9]. The main ways for the synthesis of T_8 cores are the acid or base catalysed hydrolytic polycondensation of simple chloro- or alkoxysilanes and hydroxide/fluoride catalysed rearrangement of silsesquioxane resins [6,10,11].

In this paper we report the synthesis, structural data and some properties for the acid hydrolysis product of 3-mercaptopropyltrimethoxysilane, this being octakis(3-mercaptopropyl)octasilsesquioxane (**1**). This compound, in principle, is known but could not be isolated as single crystals for X-ray diffraction study. The thiol group is useful for the chemical modification of the electrode [12], for the preparation of proton conductive membranes (thiol groups being easily converted into sulfonic acid groups by a mild oxidation) [13], for the modification of inorganic nanoparticles [14], for the synthesis of super-hydrophilic mesoporous silica via a sulfonation route [15,16] or functional xerogels [17–19].

* Corresponding author.
E-mail address: mcazacu@icmpp.ro (M. Cazacu).

http://dx.doi.org/10.1016/j.jorganchem.2015.09.025
0022-328X/

2. Experimental section

2.1. Materials

3-Mercaptopropyltrimethoxysilane (99%, $d_{20°C}$ = 1.05 g/L), and hydrochloric acid (c = 37%) were purchased from Sigma Aldrich and used as such. Methanol p.a. was acquired from Chemical Company.

2.2. Measurements

Fourier transform infrared (FT-IR) spectra were recorded using a Bruker Vertex 70 FT-IR spectrometer. Analyses were performed in the transmission mode in the 400–4000 cm^{-1} range, at room temperature, with a resolution of 2 cm^{-1} and accumulation of 32 scans. The samples were incorporated in dry KBr and processed as pellets in order to be analyzed. The NMR spectra were recorded on a Bruker Avance DRX 400 MHz Spectrometer equipped with a 5 mm QNP direct detection probe and z-gradients. Spectra were recorded in $CDCl_3$ or DMSO-d_6, at room temperature. The chemical shifts are reported as δ values (ppm) relative to the solvent residual peak. The carbon, hydrogen, and nitrogen contents were determined by standard methods. The thermogravimetric analysis was performed on STA 449F1 Jupiter NETZSCH (Germany) equipment. The measurements were made in the temperature range 20–700 °C under a nitrogen flow (50 mL/min) using a heating rate of 10 °C/min. Differential scanning calorimetry (DSC) measurements were conducted on a DSC 200 F3 Maia device (Netzsch, Germany). A mass of 15 mg of each sample was heated in pierced and sealed aluminum crucibles at a heating rate of 10 °C min^{-1}. Nitrogen atmosphere at a flow rate of 50 mL min^{-1} was used. The temperature against heat flow was recorded. The device was calibrated using indium according to standard procedures. Dynamic water vapor sorption (DVS) capacity of the samples was determined in the relative humidity (RH) range 0–90% by using the fully automated gravimetric analyzer IGAsorp produced by Hiden Analytical, Warrington (UK).

2.3. Biological activity

The antimicrobial activity was evaluated *in vitro* according to the standard methods on laboratory strains: fungi *Aspergillus niger* ATCC 53346, *Penicillium frequentans* ATCC 10110 and *Alternaria alternata* (ATCC 8741), Gram-negative bacteria *P. aeruginosa* ATCC 27813 and Gram-positive *Bacillus polymyxa* were provided by American Type Culture Collection (ATCC, USA). Sample solutions of 0.5 wt%, 1 wt% and 2 wt% concentrations were obtained by dissolution of appropriate amounts of tested compound in fixed volumes of acetone. It must be mentioned that for fungi was used a Sabouraud type agar medium supplemented with dextrose (4%, SDA) and for bacteria a Standard I nutrient agar medium, both from Merck (Germany). Microorganism's suspensions were prepared using the method of successive agar dilutions according to standard MIC and their cultivation according to standard procedures (SR-EN 1275:2006 and NCCLS guidelines). Final charge-stock inoculum was prepared as 1×10^{-4} μg/ml concentration and inoculated plates were incubated at 30 °C for 7 days. Caspafugin (small test) was used as a standard antifungal compound and Kanamycin (small test) was used for antibacterial activity. Standard compounds derived from Liofilchem Company. The MIC is read directly from the scale in terms of μg/mL at the point where the edge of the inhibition ellipse intersects the strip MIC Test Strip. The first observations were made after 48 h and finally, after 7 days of incubation, using visual, microscopy and photography analyses minimum inhibitory concentration (MIC).

2.4. X-ray crystallography

Crystallographic measurements for compound **1** were carried out with an Oxford-Diffraction XCALIBUR E CCD diffractometer equipped with graphite-monochromated Mo-Kα radiation. The crystal was placed at 40 mm from the CCD detector and 411 frames were measured each for 70 s over 1° scan width. The unit cell determination and data integration were carried out using the CrysAlis package of Oxford Diffraction [20]. The structure was solved by direct methods using Olex2 [21] software with the SHELXS [22] structure solution program and refined by full-matrix least-squares on F_o^2 with SHELXL-97 [22]. Atomic displacements for non-hydrogen, non-disordered atoms were refined using an anisotropic model. The hydrogen atoms of SH groups were found in difference-Fourier maps and refined accounting for the hybridisation of the supporting atoms and the hydrogen bonds parameters. All other hydrogen atoms were placed in geometrically calculated positions and included in the refinement process using riding model. The molecular plots were obtained using the Olex2 program [21]. The main crystallographic data together with refinement details are summarized in Table 1, while the selected bond lengths and angles can be found in Table 2.

CCDC-959470 (1) contains the supplementary crystallographic data for this contribution. These data can be obtained free of charge via www.ccdc.cam.ac.uk/conts/retrieving.html (or from the Cambridge Crystallographic Data Centre, 12 Union Road, Cambridge CB2 1EZ, UK; fax: (+44) 1223-336-033; or deposit@ccdc.ca.ac.uk).

2.5. Procedure

Preparation of octakis(3-mercaptopropyl)octasilsesquioxane, **1**: 7.46 g (0.038 mol) 3-mercaptopropyltrimethoxysilane, 250 mL methanol and 15 mL hydrochloric acid 37% were introduced in a well dried round bottom flask, in nitrogen atmosphere. The mixture was stirred 1 h and then left to rest at room temperature. Colorless

Table 1
Crystallographic data, details of data collection and structure refinement parameters for the compound **1**.

	1
Empirical formula	$C_{24}H_{56}O_{12}S_8Si_8$
Formula weight	1017.89
Temperature/K	200
Crystal system	triclinic
Space group	*P*-1
a/Å	9.6395(5)
b/Å	9.7036(6)
c/Å	13.7908(6)
α/°	74.371(5)
β/°	79.506(4)
γ/°	79.428(5)
V/Å3	1209.13(11)
Z	1
D_{calc}/mg/mm^3	1.398
μ/mm^{-1}	0.615
Crystal size/mm^3	0.02 × 0.10 × 0.15
θmin, θ max(°)	4.72 to 52
Reflections collected	10796
Independent reflections	4738 [R_{int} = 0.0307]
Data/restraints/parameters	4738/0/235
R_1[a]($I > 2\sigma(I)$)	0.0565
wR_2[b](all data)	0.1521
GOF[c]	1.057
$\Delta\rho_{max}$ and $\Delta\rho_{min}$/e/Å^3	0.59/−0.45

[a] $R_1 = \Sigma||F_o| - |F_c||/\Sigma|F_o|$.

[b] $wR_2 = \{\sum[w(F_0^2 - F_c^2)^2]/\sum[w(F_0^2)^2]\}^{1/2}$.

[c] GOF $= \{\sum[w(F_0^2 - F_c^2)^2]/(n-p)\}^{1/2}$, where n is the number of reflections and p is the total number of parameters refined.

Table 2
Selected bond lengths (Å)° and angles (°) for **1**. See Fig. 1 for atom numbering.

Si1–O1	1.614(2)
Si1–O4	1.617(2)
Si1–O5	1.618(2)
Si2–O1	1.624(3)
Si2–O2	1.617(2)
Si2–O6	1.624(3)[1]
Si3–O2	1.618(2)
Si3–O3	1.617(2)
Si3–O5	1.620(2)[1]
Si4–O3	1.616(2)
Si4–O4	1.616(2)
Si4–O6	1.620(2)
O1Si1O4	109.3(1)
O1Si1O5	109.0(1)
O4Si1O5	109.2(1)
O1Si2O2	109.0(1)
O1Si2O6	109.5(1)[1]
O2Si2O6	108.7(1)[1]
O2Si3O3	108.6(1)
O2Si3O5	108.7(1)[1]
O3Si3O5	109.2(1)[1]
O3Si4O6	108.9(1)
O4Si4O3	109.2(1)
O4Si4O6	109.0(1)
Si1O1Si2	150.0(2)
Si2O2Si3	153.1(2)
Si3O3Si4	150.8(2)
Si1O4Si4	152.3(2)
Si1O5Si3	144.9(2)[1]
Si4O6Si2	144.5(2)[1]

Symmetry code used to generate equivalent atoms: [1]1–*x*, –*y*, –*z*.

crystals, suitable for XRD were formed after one month from solution (crystals yield: 0.77 g, 16 wt%). Elemental analysis, wt%: found: C, 29.40; H, 5.97; calculated for the molecular formulas $C_{24}H_{56}O_{12}S_8Si_8$ (M = 1017.89 g/mol), %: C, 28.30; H, 5.50. IR (KBr pellet, cm^{-1}): 399w, 422vw, 474m, 536 w, 553w, 659vw, 669w, 690m, 810w, 1007m, 1109s, 1186m, 1244w, 1263m, 1306vw, 1346w, 1375w, 1408w, 1427w, 1441w, 1452w, 1630m, 1688w, 1711m, 1719m, 2855w, 2892w, 2928m, 2955w, 3408vs (Fig. 1S). ^{1}H-NMR (400.13 MHz, $CDCl_3$): 0.75 (t, J = 8 Hz, Si–CH_2–), 1.37 (t, J = 8 Hz, CH_2–CH_2–CH_2–*SH*), 1.70 (pen, J = 7.6 Hz, Si–CH_2–CH_2–), 2.54 (q, J = 7.4 Hz, Si–CH_2–CH_2–*CH_2*–SH), intensities ratio: 1:0.5:1:1 (Fig. 2S). ^{13}C NMR (100.6 MHz, $CDCl_3$): 10.82 (Si–CH_2–), 27.28 (Si–CH_2–CH_2–CH_2–SH), 27.54 (Si–CH_2–CH_2–). ^{29}Si-NMR (79.49 MHz, $CDCl_3$): –67.11 (Fig. 3S).

3. Results and discussion

3-Mercaptopropyltrimethoxysilane was hydrolyzed in presence of hydrochloric acid, at room temperature (Scheme 1) according to procedure described by Feher [23] this being one of the most used synthetic route to oligosilsesquioxanes and their homo derivatives [3]. Over time, in static regime, cubic silsesquioxane separated in crystalline form. The elemental analysis values for the obtained compound corresponds to the closed cubes, with mercapto functional groups, as was emphasized by the other methods.

Vibrational spectroscopy has been used extensively for the characterization of T_8 compounds, particularly for checking the characteristic Si–O–Si band that is usually strong and occurs at ca. 1100 cm^{-1}, but it is also broad, this explaining various values reported by different authors [6]. In FTIR spectrum of the compound **1** (Fig. 1S), a low-intensity absorption band at 2554 cm^{-1} is assigned to ν(SH) proving the existence of thiol groups in structure [24]. The

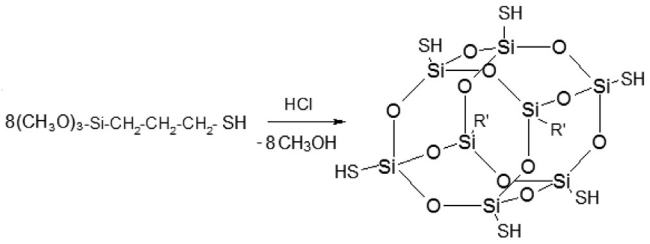

Scheme 1. Hydrolysis reaction leading to octasilsesquioxane **1**.

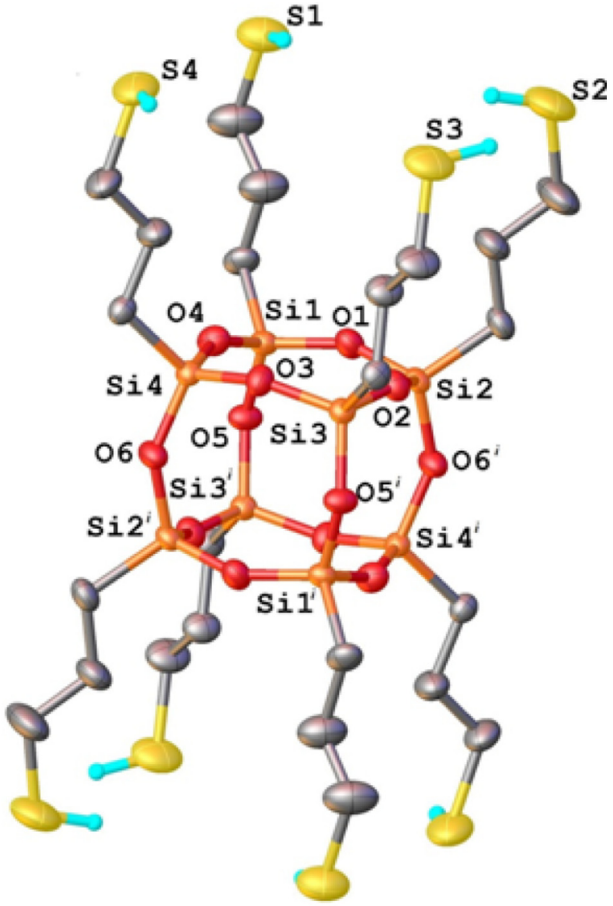

Fig. 1. X-ray molecular structure of $[HS(CH_2)_3]_8Si_8O_{12}$ (**1**). Non-relevant hydrogen atoms are not shown for clarity. Thermal ellipsoids are drawn at 50% probability level.

bands around 3436 and 1624 cm^{-1} indicate the presence of the water molecules in compound. CH stretching of the propyl group appears as intense one at 2929 cm^{-1}. The most prominent bands are at 1107 and 474 cm^{-1}, these being assigned to asymmetric and symmetric stretching of Si–O–Si bond. The peaks at 690 and 1263 cm^{-1} belong to C–Si bond. The peaks at around 1427 cm^{-1} come from asymmetric deformations of C–H in propyl group. ^{1}H NMR spectrum of the compound shows peaks corresponding and in intensity ratios as proposed structure (Fig. 2S), while the peak in ^{29}S NMR (67.22 ppm) is characteristic for cubic architecture (Fig. 3S).

3.1. Crystal structure analysis

The X-ray molecular structure of compound 1 is depicted in Fig. 1. The $[HS(CH_2)_3]_8Si_8O_{12}$ (**1**) molecule is generated by the

crystallographic center of symmetry, which is located in the center of octasilsesquioxane cage. The single crystal structure showed the molecule **1** adopts a "squashed" configuration for the eight 3-mercaptopropyl substituents and the Si_8O_{12} cube is elongated. This is evidenced by the comparison of Si1O1Si2 150.0(2)°, Si3O3Si4 150.8(2)° with Si1O5Si3^i 144.9(2)°, Si4O6Si2^i 144.5(2)° angles (see Table 2) and of Si1 … Si2 3.128(1) Å, Si3 … Si4 3.129(1) Å with Si1 … Si3^i 3.087(1) Å, Si4 … Si2^i 3.090(1) Å distances. At the same time, the Si–O, Si–C and C–S bond lengths fall in the narrow range 1.614(2) ÷ 1.624(2) Å, 1.835(3) ÷ 1.838(3) Å and 1.786(3) ÷ 1.810(3) Å, respectively and do not exceed those observed for other silsesquioxanes. It should be also noted, that although Si–O–Si angles vary in the relative wide range, the O–Si–O angles are very close to that of ideal tetrahedral geometry (Table 2). The X-ray molecular structure of **1** demonstrate the Si_8O_{12} cage do not corresponds to the ideal cubic arrangement as observed for similar substituted $Si_8O_{12}R_8$ compounds [25–28]. Adjacent $[HS(CH_2)_3]_8Si_8O_{12}$ molecules are associated into one-dimensional supramolecular chains (Fig. 2) due to the intermolecular S–H … S hydrogen bonds (see Table 3). The crystal structure is built from the parallel packing of 1D supramolecular architecture running along *c* axis, as shown in Fig. 3.

Overall dimensions expressed as O–O distance within the cage (inner diameter) and R–R distance (outer diameter) in cubic polyhedral structure, estimated on the basis of the crystallographic data (Fig. 4S), were 0.54, 1.63 nm. The nanometric size of these hybrid organic-inorganic frameworks makes them ideal building blocks for nanocomposites permitting the reinforcement of the polymeric matrix at molecular level. Besides the rigidity and improved thermal and mechanical properties conferred by the silica core, the functional groups attached to the silicon atoms can induce specific properties (compatibility, polarizability, hydrophobicity or hydrophilicity, etc.).

Table 3
H-bonds parameters for compound **$[HS(CH_2)_3]_8Si_8O_{12}$** (**1**).

D-H … A	Distance, Å			Angle D-H … A, deg	Symmetry code
	D-H	H … A	D … A		
S1–H … S3	1.20	2.92	4.035(2)	153.7	1 − *x*, −*y*, 1 − *z*
S2–H … S3	1.19	2.93	4.068(2)	159.6	1 − *x*, −*y*, 1 − *z*
S3–H … S4	1.20	2.94	4.008(2)	147.8	1 − *x*, −*y*, 1 − *z*
S4–H···S2	1.21	2.91	4.054(3)	158.2	1 − *x*, −*y*, 1 − *z*

3.2. The thermal behavior

The thermal stability of POSS can be as high as 500 °C, but varies considerably in dependence on the stability of the organic group. The most detrimental substituents are nucleophilic groups, such as amines, which aid in the breaking of siloxane bonds, particularly at higher temperatures [1]. In our case, the compound contains nucleofilic –SH group. However, the mercapto functionalized compound begins to decompose in nitrogen atmosphere at 307 °C and the process occurs in two stages with a total weight loss of 64 wt% (Fig. 4, Table 4).

Two endothermic transitions were observed. First, a major melting point (T_{m1}) was determined at 162 °C with an enthalpy value (ΔH_{m1}) of 0.7 J g^{-1} and a minor enthalpy transition (ΔH_{m2} = 0.5 J g^{-1}) at T_{m2} = 105 °C. The two endothermic processes determined the apparition of a major (T_{c1} = 133 °C; ΔH_{c1} = −0.6 J g^{-1}) and a minor crystallization transition (T_{c2} = 101 °C; ΔH_{c2} = −0.2 J g^{-1}). As X-ray diffraction showed, structure of crystal **1** consists in one-dimensional supramolecular chains formed as a result of molecules association through intermolecular S–H···S hydrogen bonds giving a behavior somewhat similar with that for polymers and thus not very well defined transitions. The minor enthalpy transitions on both heating and cooling segments were attributed to a minor structural reordering

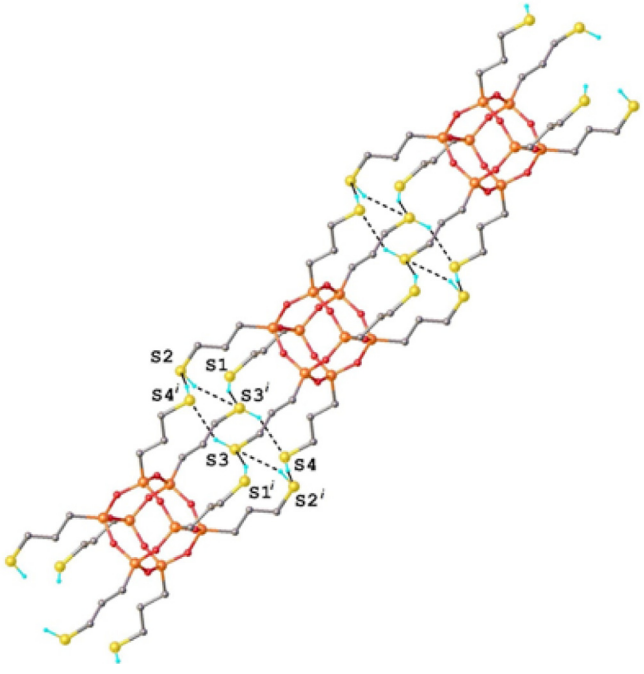

Fig. 2. The view of 1D supramolecular chain in the crystal structure **1**. Symmetry code used to generate equivalent atoms: $^{i)}$1 − *x*, −*y*, 1 − *z*.

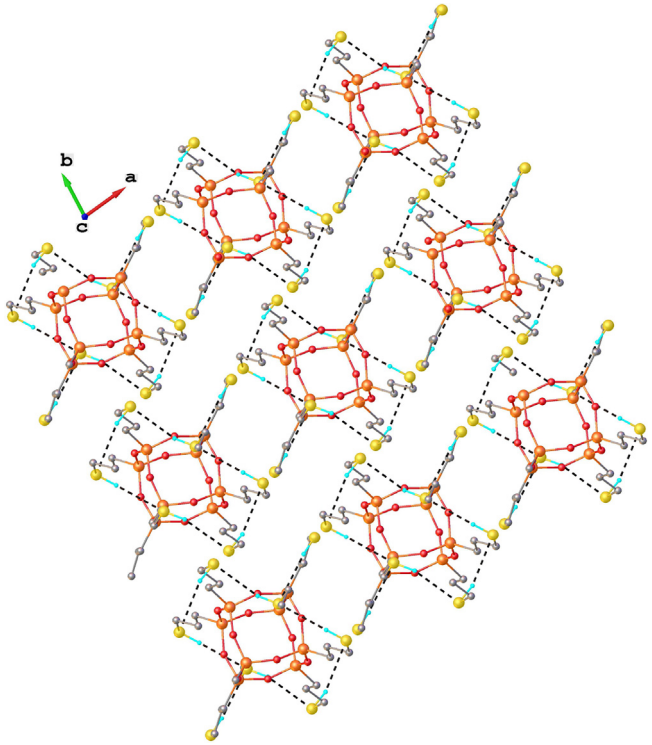

Fig. 3. Crystal structure of **1**, viewed along *c* axis.

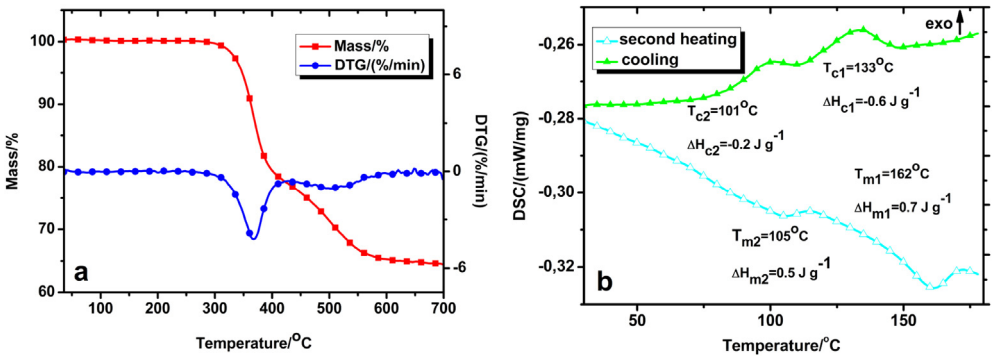

Fig. 4. TG-DTG (left) and DSC (a-second heating; b-cooling) (right) curves for the compound **1** recorded in nitrogen atmosphere.

Table 4
Thermal decomposition characteristics.

Sample	Step	T (°C)			W_m (%)	W_{rez} (%)
		T_i	T_{max}	T_f		
1	I	307	368	386	22	64
	II	433	503	548	14	

T_i – initial thermal degradation temperature; T_{max} – temperature that corresponds to the maximum rate of decomposition for each stage evaluated from the peaks of the DTG curves; T_f – final thermal degradation temperature; W_m – mass loss rate corresponding to the T_{max} values; W_{rez} – percentage of residue remained at the end of thermal degradation (700 °C).

or rotation of the propylic entities untethered to the POSS cage [29]. The terminal groups of the alkyl entities may undergo out of plane twisting or kinking moves leading to a minor structural disorder. Similar observations were reported in the literature for POSS cages with small branched or linear alkyl chains as arm substituents [30–33].

3.3. Moisture behavior

The moisture stability of the isolated POSS was evaluated by water vapor sorption analysis in dynamic regime. Sorption–desorption isotherms were registered at three temperatures: 25 °C and 35 °C (Fig. 5).

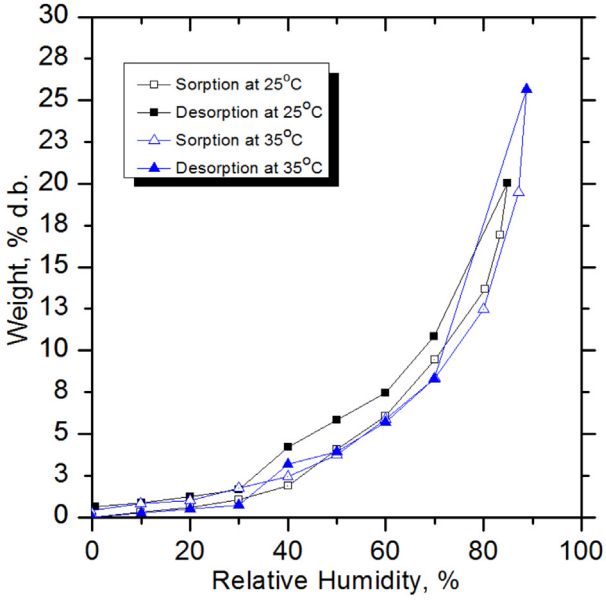

Fig. 5. Water vapor sorption isotherms registered in dynamic regime at 25 and 35 °C.

The compound shows a moisture sorption capacity of 20 wt% at a relative humidity (RH) of 90 %, at room temperature. As the temperature increases at 35 °C, the maximum sorption capacity reaches 25.7% at 90% RH. After desorption, the sample returns to the initial mass without significant changes. The high value of the water vapor sorption is in contradiction with zero value for the solvent accessibility estimated on the basis of crystallography data. Otherwise, the crystallographic analysis did not reveal the presence of solvate water or other solvent molecules in crystal structure **1**. Perhaps this sorption is based in fact on the destruction of intermolecular hydrogen bonds and replacing them with others, which are formed with more polar water molecules (the electronegativity difference in O–H group is 1.4 as compared with 0.4 in S–H group). This could explain the increased vapor sorption value as the temperature increases.

3.4. Biological activity

Some of the compounds containing thiol groups (thiodiazoles, substituted 1,3,4-thiadiazolium-5-thiolates, mercaptotriazole, 1,3,4-oxadiazoles) proved often effective as antibacterian and antifungal therapeutics by forming mixed disulphide with thiol-bearing enzymes and thus inhibiting enzymatic pathways regulated by these proteins [34]. Their lipophilicity enhances this effect [35]. Our compound possessing a high content of sulfhydryl groups (eight groups per molecule) was evaluated from point of view of antibacterial and fungicidal activity by performing *in vitro* tests against pure culture of three fungi species (*Aspergillus niger*, *P. frequentans*, *A. alternata*) and against both Gram-negative (*P. aeruginosa*) and Gram-positive (*B. polymyxa*) bacteria. The minimum inhibitory concentration (MIC) values of the compound are summarized in Table 5. According to these data, the compound **1** has been shown to be potentially biologically active, MIC values for fungal species is 13 μg/ml and 12 μg/ml for species of bacteria. However, this activity is lower as compared with reference compounds, Caspafungin (MIC values for fungal species is 3.6 μg/ml) and Kanamycin (MIC is 5.5 μg/ml species of bacteria) but is higher as compared with values reported in literature for example, in the case of thiodiazole aromatics against *Staphylococcus aureus*, in the range 31–62 μg/ml [34] or *Candida albicans* and *Saccharomyces cerevisiae*, with minimum fungicidal concentration (MFC) values in the range 12.5–61 μg/ml [36]. It can be observed a higher antibacterial as compared with antifungal activity of this compound.

Table 5
The results of the antifungal and antimicrobial activity tests for the compound **1**.

Sample	MIC (μg/ml)				
	Fungi			Bacteria	
	Aspergillus niger ATCC 53346	*Penicillium frequentans* ATCC 10110	*Alternaria alternate* ATCC 8741	Bacillus sp. ATCC 15970	*Pseudomonas aeroginosa* ATCC 27813
	Sample concentration, wt%				
	2	2	2	2	2
1	13	13	12,5	12	12
Caspofungin[a]	3.60	3.60	3.7	–	–
Kanamycin[a]	–	–	–	5,5	5,5

[a] Standard compound.

4. Conclusion

The acid hydrolysis product of 3-mercaptopropyltrimethoxysilane (**1**) was isolated and its structure was determined by spectral analysis and X-ray single crystal diffraction. The SH group was preserved as such in the harsh conditions of the hydrolysis. An elongation was observed in inner cage of the structure. The packing model of the compound **1** consists in one-dimensional supramolecular chains. The silsesquioxane containing mercapto group was found to have a good thermal stability, showed biological activity but adsorbs a high amount of humidity.

Acknowledgments

This work was supported by a grant of the Ministry of National Education, CNCS – UEFISCDI, project number PN-II-ID-PCE-2012-4-0261.

Appendix A. Supplementary data

Supplementary data related to this article can be found at http://dx.doi.org/10.1016/j.jorganchem.2015.09.025.

References

[1] C. Hartmann-Thompson, Applications of Polyhedral Oligomeric Silsesquioxanes, in: Advances in Silicon Science, Springer, vol. 3, Dordrecht Heidelberg London New York, 2011, p. 24.
[2] S. Sulaiman, Synthesis and Characterization of Polyfunctional Polyhedral Silsesquioxane Cages, PhD Dissertation, University of Michigan, 2011.
[3] Z. Zhang, G. Liang, J. Appl. Polym. Sci. 103 (2007) 2608–2614.
[4] S. Fabritz, S. Hörner, O. Avrutina, H. Kolmar, Org. Biomol. Chem. 11 (2013) 2224–2236.
[5] G. Gerritsen, Silsesquioxane Lego Chemistry: Catalytic Receptor Ensembles for Alkene Epoxidation, Technische Universiteit Eindhoven, 2011.
[6] D.B. Cordes, P.D. Lickiss, F. Rataboul, Chem. Rev. 110 (2010) 2081–2173.
[7] D.M.L. Goodgame, S. Kealey, P.D. Lickiss, J. Mol. Struct. 890 (2008) 232–239.
[8] T. Ceyhan, M. Yuksek, H.G. Yaglıoglu, B. Salih, M.K. Erbil, A. Elmal, O. Bekaroglu, Dalton Trans. 18 (2008) 2407–2413.
[9] E. Ayandele, B. Sarkar, P. Alexandridis, Nanomaterials 2 (2012) 445–475.
[10] M. Koželj, B. Orel, Dalton Trans. 42 (2012) 9432–9436.
[11] P.P. Pescarmona, An Exploration of Silsesquioxanes and Zeolites Using High-speed Experimentation, PhD Dissertation, Technische Universiteit Delft, 2003.
[12] I. Cesarino, E. Tadeu, G. Cavalheiro, Mater. Res. 11 (2008) 465–469.
[13] H. Lee, S.B. Park, M.H. Oh, K. Cho, Y. Park, J. Korean Phys. Soc. 56 (2010) 1215–1222.
[14] A. Tsukamoto, T. Isobe, J. Mater. Sci. 44 (2009) 1344–1350.
[15] Y.K. Oh, L.Y. Hong, Y. Asthana, D.P. Kim, J. Ind. Eng. Chem. 12 (2006) 911–917.
[16] D. Margolese, J.A. Melero, S.C. Christiansen, B.F. Chmelka, G.D. Stucky, Chem. Mater 12 (2000) 2448–2459.
[17] Y.L. Zub, N.V. Stolyarchuk, I.V. Melnyk, A.A. Chuiko, A. Dabrowski, M. Barczak, Mendeleev Commun. 15 (2005) 168–170.
[18] M. Barczak, A. Dabrowski, The 65th Birthday of Professor Roman Leboda, AA LXIV, Annales Universitatis Mariae Curie – Skłodowska, Lublin – Polonia, 2009, pp. 1–10.
[19] X. Wang, D. Li, F. Yang, H. Shen, Z. Li, D. Wu, Polym. Chem. 4 (2013) 4596–4600.
[20] CrysAlis RED, Oxford Diffraction Ltd, 2003. Version 1.171.34.76.
[21] O.V. Dolomanov, L.J. Bourhis, R.J. Gildea, J.A.K. Howard, H. Puschmann, J. Appl. Crystallogr. 42 (2009) 339–341.
[22] G.M. Sheldrick, A short history of SHELX, Acta Cryst. A64 (2008) 112–122.
[23] F.J. Feher, K.D. Wyndham, D. Soulivong, F. Nguyen, J. Chem. Soc. Dalton Trans. (1999) 1491–1497.
[24] M. Barczak, A. Dabrowski, J. Ryczkowski, S. Pasieczna-Patkowska, Eur. Phys. J. Spec. Top. 154 (2008) 301–304.
[25] A.V. Zakharov, S.L. Masters, D.A. Wann, S.A. Shlykov, G.V. Girichev, S. Arrowsmith, D.B. Cordes, P.D. Lickiss, A.J.P. White, Dalton Trans. 39 (2010) 6960–6966.
[26] P.D. Lickiss, F. Rataboul, Adv. Organomet. Chem. 57 (2008) 1–116.
[27] G. Li, C.U. Pittman Jr., in: A.S. Abd-El-Aziz, C.E. Carraher, C.U. Pittman Jr., M. Zeldin (Eds.), Macromolecules Containing Metal and Metal-like Elements, vol. 4, Wiley, Weinheim, Germany, 2005, pp. 79–131. Group IVA Polymers.
[28] N.L. Dias Filho, Fa C.M. Portugal, J.M.F. Nogueira, P. Brandão, V. Felix, P.D. Vaz, C.D. Nunes, L.F. Veiros, M.J. Villa de Brito, M.J. Calhorda, Organometallics 31 (2012) 4495–4503.
[29] E.L. Heeley, D.J. Hughes, Y. El Aziz, I. Williamson, P.G. Taylor, A.R. Bassindale, Phys. Chem. Chem. Phys. 15 (2013) 5518–5529.
[30] M.J. Abad, L. Barral, D.P. Fasce, J.J. Williams, Macromolecules 36 (2003) 3128–3135.
[31] G.M. Poliskie, T.S. Haddad, R.L. Blanski, K.K. Gleason, Thermochim. Acta 438 (2005) 116–120.
[32] G. Croce, F. Carniato, M. Milanesio, E. Boccaleri, G. Paul, W. Van Beek, L.W. Marchese, Phys. Chem. Chem. Phys. 11 (2009) 10087–10094.
[33] F.X. Perrin, T.B. Viet Nguyen, A. Margaillan, Eur. Polym. J. 47 (2011) 1370–1382.
[34] M.A. Ghannoum, N.F. Eweiss, A.A. Bahajaj, M.A. Qureshi, Microbios 37 (1983) 151–159.
[35] P. Domenico, R.J. Salo, S.G. Novick, P.E. Schoch, K.V. Horn, B.A. Cunha, Antimicrob. Agents Chemother. (1997) 1697–1703.
[36] K. Baranski, T.J. Bardos, A. Bloch, T.I. Kalman, Biochem. Pharmacol. 18 (1969) 347–358.